

Electronic structure of copper overlayers on the (100) and (111) surfaces of tungsten

G. A. Gaudin

Department of Physics, University of Toronto, Toronto, Ontario, Canada M5S 1A7

M. J. G. Lee

Department of Physics and Scarborough College, University of Toronto, Toronto, Ontario, Canada M5S 1A7

(Received 14 July 1993; revised manuscript received 10 November 1993)

Field-emission and photofield-emission measurements of the surface density of electronic states have been carried out for copper chemisorbed on the (100) and (111) facets of a thermally annealed tungsten field emitter, in the range of temperature, and coverage where the adsorbed atoms form spatially homogeneous overlayers. Such overlayers are found to modify the intrinsic surface states of the substrate, and to introduce, on the (100) facet, additional features in the surface density of states. The observation of a final-state effect in surface photofield emission is reported, demonstrating that this technique can provide useful information on the surface density of states of an adsorbed overlayer in the energy range between the Fermi level and the vacuum level. The present work offers insight into earlier conflicting results concerning the effect of adsorbed copper on the intrinsic surface states of tungsten surfaces.

I. INTRODUCTION

Most studies of the electronic structures of noble metals chemisorbed on tungsten have focused on the W(100) surface. This has stemmed from interest in the effect of adsorbates in suppressing the surface state observed by Swanson and Crouser¹ as a strong deviation from free-electron behavior in the field-emission total energy distribution (TED) for the clean W(100) surface. This state, which lies approximately 0.3 eV below the Fermi level, is also seen in surface photofield emission, i.e., when the polarization vector of the incident light has an appreciable component normal to the emitting surface (p polarization),^{2,3} and in angle-resolved ultraviolet photoemission spectroscopy (ARUPS) at normal emission.⁴ It is believed to originate from a band of even-symmetry surface states that exists at zero transverse wave vector, i.e., at the point $\bar{\Gamma}$ at the center of the surface Brillouin zone.^{5,6} While overlayers of chemisorbed noble metals have generally been found to suppress the surface state both in field emission⁷⁻⁹ and in ARUPS,¹⁰ significant differences exist in the observed dependence on coverage between the field-emission and photoemission data, and also between field-emission data obtained by different workers. The present research was motivated by the need to resolve the discrepancies between the results of previous workers on W(100), and to supplement the sparse experimental data reported for noble-metal overlayers on other tungsten surfaces.¹¹⁻¹³

The present paper investigates the electronic structure of copper chemisorbed at 300 K on the (100) and (111) facets of a thermally annealed tungsten field emitter by exploiting the selective sensitivity of field emission¹⁴ and photofield emission in p polarization² to the density of electronic states in the vicinity of the surface. Surface photofield emission, which has not previously been used to study noble metals adsorbed on tungsten, provides spectroscopic information not only below the Fermi level,

complementary to that provided by field emission, but also in the energy range between the Fermi level and the vacuum level. The measurements are restricted to the range of coverage where the adsorbed atoms form spatially homogeneous overlayers; below one monolayer on the (100) facet and below two monolayers on the (111) facet. At higher coverages, copper atoms are known to aggregate to form stable islands, yielding spatially inhomogeneous overlayers.^{15,16}

It is found that adsorbing spatially homogeneous copper overlayers substantially modifies the surface electronic structure of the tungsten substrates. Furthermore, additional features attributed to the electronic structure of the adsorbate emerge in the surface density of states during the growth of overlayers on the (100) facet, but not on the (111) facet. These findings are discussed in the light of previous work, and possible reasons for discrepancies are offered. The present study also reports the observation of structure in the surface density of states at the final-state energy in photofield emission, demonstrating that photofield emission can provide useful information on the surface density of states of adsorbed overlayers between the Fermi level and the vacuum level.

The remainder of this paper is organized as follows. Section II briefly describes the apparatus and outlines the procedures for collecting and analyzing the data. Results are reported in Sec. III and discussed in Sec. IV, while conclusions are summarized Sec. V. Work on the electronic structure of spatially inhomogeneous copper overlayers is reported elsewhere.¹⁷

II. EXPERIMENTAL CONSIDERATIONS

The apparatus for preparing the adsorption system under study¹⁵ and the spectrometer for measuring the TED's in field emission and in photofield emission^{18,19} have been described elsewhere. A $\langle 110 \rangle$ -oriented

tungsten field emitter is mounted on a sample positioner in front of a fluorescent conducting screen. The field emitter is grounded, and a positive potential of several kilovolts is applied to the screen. Field-emitted electrons are accelerated towards the screen where they impact to produce the characteristic field-emission pattern of the emitter tip. Emission from a particular tip facet is selected by electrostatically deflecting the electrons until the corresponding region of the pattern is aligned over a small probe hole in the center of the screen. An energy analyzer consisting of two 127° cylindrical analyzers in tandem measures the TED of the current passing through the probe hole with a resolution of 60 meV. The evaporation source for the deposition system and the spectrometer are enclosed within a stainless-steel UHV chamber to minimize contamination of the tip surface by residual gases. For studies of photofield emission, a krypton-ion laser and focusing system located outside the vacuum chamber produce a Gaussian distribution of irradiance at the tip with a waist radius of about 4 μm .

TED data in field emission and in photofield emission were obtained by sweeping the field-emitter bias voltage through 80–100 equally spaced channels of width 24 mV spanning the appropriate energy ranges. At each channel the bias voltage was allowed to stabilize for 10 μs , then electrons were counted for 0.4 ms. The sweep sequence was repeated until adequate statistics had been achieved. When collecting photofield-emission data, the sweeps over the photofield-emission TED were always interleaved with sweeps over the field-emission TED. Laser illumination of the tip was maintained during the field-emission sweeps to avoid temperature differences due to laser heating. All photofield-emission measurements were made using *p*-polarized light at a large angle of incidence to ensure that surface photoexcitation was dominant.²⁰

As the first step in a typical experiment, TED data in field emission and, if required, photofield emission were obtained from the clean facet. Copper was then deposited onto the field emitter at room temperature (300 K) with a potential difference applied between the tip and the screen. The current passing through the probe hole due to field emission from the facet was monitored, and deposition was stopped when the facet had been exposed to the desired amount of copper. The copper flux was measured using a thin-film thickness monitor both before and after deposition to check whether any overall drift had occurred. When all measurements were complete, the absorbed copper was removed by repeatedly flashing the tip to incandescence.

The TED in field emission decreases exponentially both below the Fermi energy E_F , due to the increasing thickness of the surface-potential barrier through which electrons with lower energy must tunnel, and above E_F , due to the decreasing occupation probability of electronic states as governed by the Fermi-Dirac distribution function. The TED in photofield emission in *p*-polarized light has a similar form except that the peak occurs near $E_F + \hbar\omega$, where $\hbar\omega$ is the photon energy. In addition, both TED's are broadened by the finite resolution of the energy analyzer. In order to remove these contributions,

and thereby extract the energy dependence from the surface density of states, all TED data are presented in the form of enhancement factors, defined by

$$R(E) = \frac{j(E)}{j_0(E)\Delta(E)} \quad (1)$$

In this expression $j(E)$ denotes the experimental TED, $j_0(E)$ the TED for a hypothetical free-electron metal with a one-dimensional classical image potential barrier, and $\Delta(E)$ the resolution function of the energy analyzer. $j_0(E)$ is calculated from the result of Young²¹ for field emission and from the surface-photoexcitation result of Schwartz and Cole²² for photofield emission in *p*-polarized light using transmission probabilities derived from an exact numerical solution of the Schrödinger equation²³ for the image potential barrier. The effects of the finite energy resolution of the analyzer are modeled by convolving $j_0(E)$ with $\Delta(E)$. $\Delta(E)$ is ideally a delta function, but imperfections in the electron optics broaden it to yield an almost Gaussian distribution.¹⁸

The calculation of $j_0(E)$ requires appropriate values for the work function ϕ and the electric-field strength $F = \beta V$, where the field factor β represents the effective curvature of the tip surface, and V is the potential difference applied between the tip and the screen. The clean-surface values of ϕ were taken from previous measurements of the absolute work function on tungsten surfaces of macroscopic size to be 4.64 eV for the (100) facet and 4.50 eV for the (111) facet.²⁴ β for a given facet was calculated from the measured dependence of the total (energy-integrated) field-emission current I on V , using the assumed value of ϕ in a finite-temperature extension of the Fowler-Nordheim equation.²⁵ $R(E)$ involves an undetermined normalizing constant because neither the area of the emitting surface sampled by the probe hole nor the collection efficiency of the energy analyzer was determined in the present work. The effect of this constant is removed by plotting $\ln R$ as a function of E .

The value of ϕ at a given copper coverage θ was obtained from a calibration of ϕ versus θ determined in a separate experiment.¹⁶ For each facet, ϕ was calculated from field emission I - V data obtained at several values of θ by using the value of β obtained for the clean facet in the finite-temperature Fowler-Nordheim equation. That β is independent of coverage was established on the (100) facet by comparing the resulting ϕ versus θ calibration with previous data for copper adsorption on macroscopic W(100) surfaces,^{26,27} for which the problem of determining β does not arise. The calibration was found to be in good agreement with the macroscopic-surface data, justifying the assumption of a coverage-independent β on the (100) facet. To the best of the present authors' knowledge, no previous measurements of ϕ versus θ have been reported for copper on macroscopic W(111) surfaces. Accordingly, the coverage independence of β on the (111) facet was verified by measuring ϕ and β independently. This was accomplished by obtaining I - V data in both field emission and photofield emission at several values of θ and analyzing these data using a procedure that has been described elsewhere.²⁵ It was found

that, over the range of coverage investigated, β deviated by not more than 2% from the value obtained for the clean (111) facet.¹⁶ Thus, on the (111) facet, the assumption of a coverage-independent β is also reasonable.

III. RESULTS

A. Enhancement factors for copper overlayers on the W(100) surface

Figure 1 shows how the field-emission enhancement factor for the (100) facet changes as a function of the coverage θ of copper adsorbed at 300 K. Figures 2–4 show the corresponding changes in the photofield-emission enhancement factors at photon energies of 2.604, 3.049, and 3.536 eV, respectively. Data are given only for the range of coverage where the copper overlayers are spatially homogeneous, i.e., where island formation does not occur ($\theta < 1$). The prominent peak in each clean surface ($\theta=0$) curve is due to the even-symmetry band of surface states that exists at $\bar{\Gamma}$.^{5,6} Previous measurements of the field-emission enhancement factor²⁸ have also revealed a small peak approximately 0.75 eV below E_F , which has been attributed^{5,6} to a lower-energy, odd-symmetry band of surface states that does not exist at $\bar{\Gamma}$. In the present data, field emission from this lower-energy band is not observed as a distinct peak, but may be responsible for the broadening observed on the low-energy side of the main peak in the $\theta=0$ curve of Fig. 1. The lower-energy structure has a small amplitude because the surface-potential barrier discriminates exponentially against the transmission of electrons with nonzero transverse wave

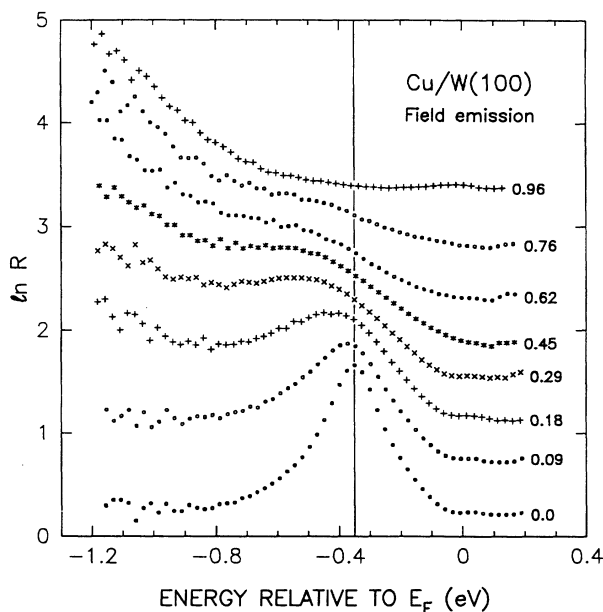


FIG. 1. Field-emission enhancement factor as a function of copper coverage θ on the W(100) facet at 300 K. Each curve is labeled by the appropriate value of θ expressed in monolayers. The curves have been displaced vertically for clarity. The vertical line marks the energy of the peak (-0.35 eV) for the clean surface.

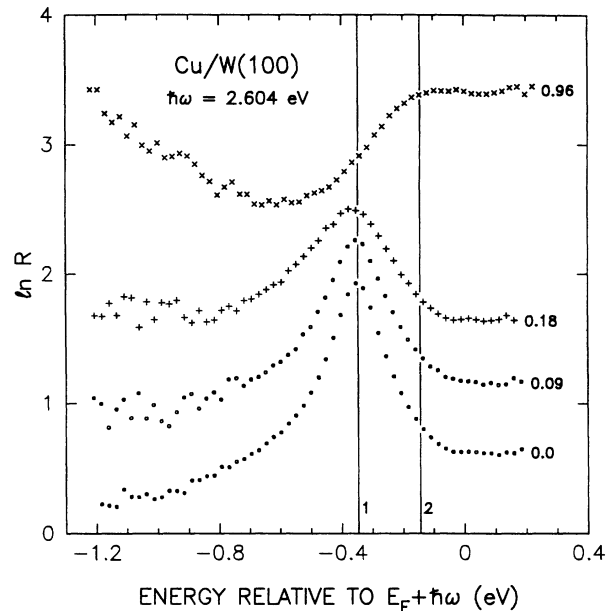


FIG. 2. Enhancement factor in photofield emission in p polarization for $\hbar\omega=2.604$ eV as a function of copper coverage θ on the W(100) facet at 300 K. The plotting conventions are defined in the caption to Fig. 1. The vertical line 1 marks the energy (-0.35 eV) of the peak for the clean surface, while the vertical line 2 marks the energy (-0.12 eV) of additional structure at $\theta=0.96$ monolayers.

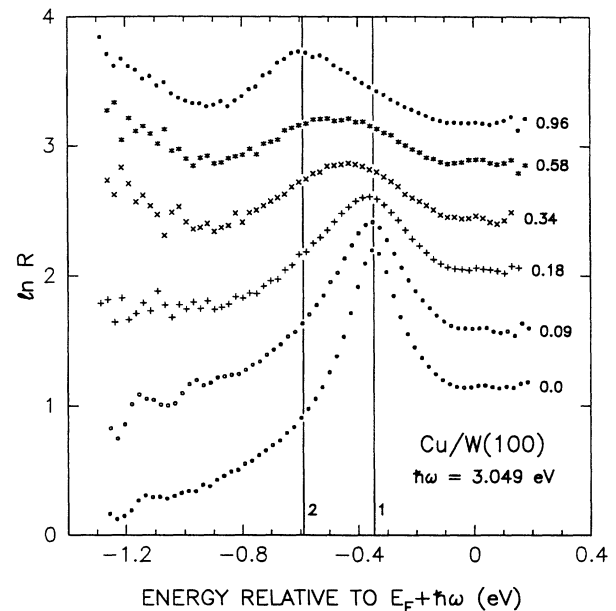


FIG. 3. Enhancement factor in photofield emission in p polarization for $\hbar\omega=3.049$ eV as a function of copper coverage θ on the W(100) facet at 300 K. The plotting conventions are defined in the caption to Fig. 1. The vertical line 1 marks the energy (-0.35 eV) of the peak for the clean surface, while the vertical line 2 marks the energy (-0.58 eV) of additional structure at $\theta=0.96$ monolayers.

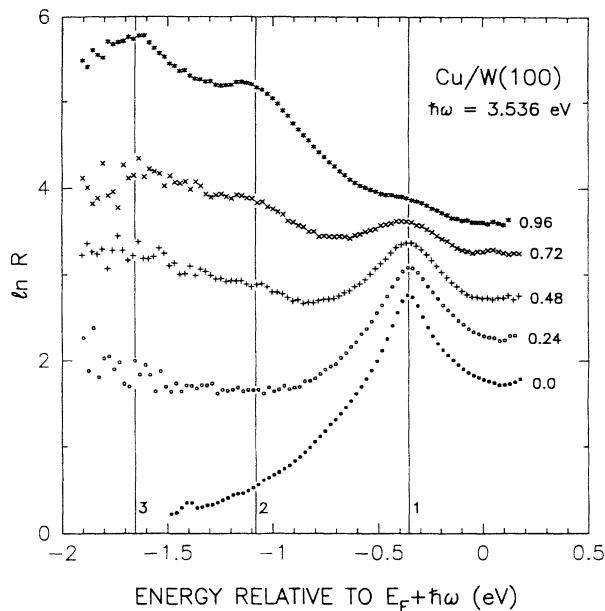


FIG. 4. Enhancement factor in photofield emission in p polarization for $\hbar\omega = 3.536$ eV as a function of copper coverage θ on the W(100) facet at 300 K. The plotting conventions are defined in the caption to Fig. 1. The vertical line 1 marks the energy (-0.35 eV) of the peak for the clean surface, while the vertical lines 2 and 3 mark the energies (-1.08 and -1.65 eV) of additional structures at $\theta = 0.96$ monolayers.

vectors over the energy range accessible in field emission. No evidence for emission from the lower-energy band is seen in the $\theta = 0$ photofield-emission curves. This is perhaps surprising because the barrier transmits electrons with larger transverse wave vectors at the final-state energies involved, especially for $\hbar\omega = 3.536$ eV, than in field emission. It has been suggested² that the lower-energy band is not observed in photofield emission using p -polarized light because only the component of the electromagnetic vector potential parallel to the surface can couple to states of odd symmetry.

The W(100) surface-state peak observed 0.35 eV below $E_F + \hbar\omega$ gradually decreases in amplitude as the coverage θ of copper increases, and is detected only in photofield emission for $\hbar\omega = 3.536$ eV (Fig. 4) when θ reaches 0.96 monolayers. In field emission, the peak appears to broaden asymmetrically and shift to lower energy as θ increases, whereas in the photofield-emission enhancement factors it broadens without an appreciable shift in energy. The behavior in field emission is partly due to the more negative slope of the background upon which the peak is superimposed. However, it might also reflect differences in the sensitivity of field emission from the lower- and higher-energy bands of surface states (the first of which does not yield a resolvable peak in the present data) to adsorbed copper. No such effect would be expected in the photofield-emission enhancement factors because the lower-energy band makes no contribution to the emission current.

At sufficiently high coverage, the enhancement factors of Figs. 1–4 reveal additional structures, which grow in strength as θ approaches one monolayer. When enhancement factors for a series of photon energies are plotted as a function of energy relative to $E_F + \hbar\omega$ ($\hbar\omega = 0$ indicates field emission), initial-state structures in the various curves are aligned. Conversely, when they are plotted as a function of energy relative to E_F , final-state structures are aligned. Therefore, in order to identify initial (final)-state structure in the different curves, it is helpful to plot them as a function of energy relative to $E_F + \hbar\omega$ (E_F).

Figures 5 and 6 show enhancement factors at $\theta = 0.96$ monolayers plotted as a function of energy relative to $E_F + \hbar\omega$ and to E_F , respectively. Field-emission data are not included in Fig. 6, since the energy range spanned by the field-emission TED at 300 K does not appreciably overlap the range spanned by the photofield-emission TED for $\hbar\omega \geq 1.916$ eV. Figure 5 shows that the weak bump at the initial-state energy -0.33 eV (marked by the vertical line labeled 1) in the curve for $\hbar\omega = 3.536$ eV does not line up with any corresponding structure in the other curves. This might be construed as evidence against this bump being identified with emission from the higher-energy band of W(100) surface states. The enhancement factors are derived from experimental TED's in which any energy dependence due to the density of states at the emitting surface is superimposed upon the energy dependence of the transmission probability at the surface potential barrier. In both field emission and photofield

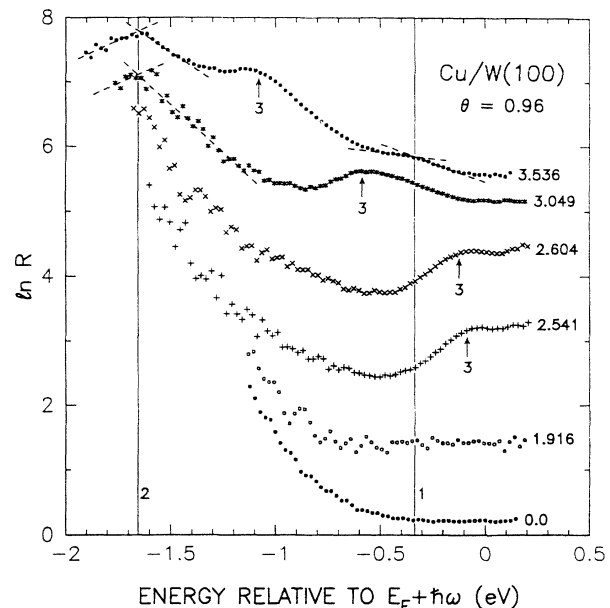


FIG. 5. Enhancement factors in field emission and in photofield emission in p polarization for 0.96 monolayers of copper chemisorbed on the W(100) facet at 300 K. Each curve is labeled by the appropriate photon energy expressed in eV. The curves have been displaced vertically for clarity. The vertical lines mark the mean energies of qualitatively similar structures (-0.33 eV for line 1 and -1.65 eV for line 2). The vertical arrows 3 mark structures that do not line up with comparable structure in any other curve.

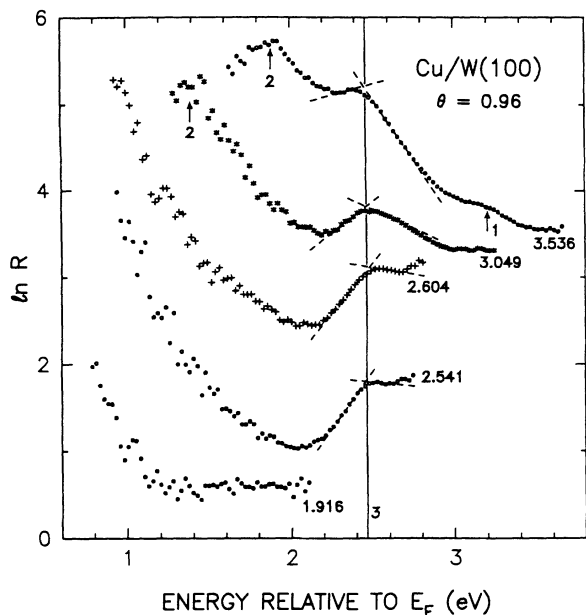


FIG. 6. Enhancement factors in photofield emission in p polarization for 0.96 monolayers of copper chemisorbed on the W(100) facet at 300 K. The plotting conventions are defined in the caption to Fig. 5. The vertical line 3 marks the mean energy (2.46 eV) of qualitatively similar structures. The vertical arrows 1 and 2 mark structures that do not line up with comparable structures in any other curve.

emission for sufficiently low $\hbar\omega$, the emitted electrons tunnel well below the peak of the barrier where the transmission probability varies exponentially as a function of electron energy. By contrast, for $\hbar\omega$ sufficiently high that the electrons pass over the peak of the barrier, the transmission probability in photofield emission will be essentially independent of energy. It follows, therefore, that the surface-state peak may be absent in field emission and photofield emission for $\hbar\omega \leq 3.049$ eV because it is concealed by a more rapid energy dependence of the transmission probability.

Figure 5 also shows that qualitatively similar structures in the curves for $\hbar\omega = 3.049$ and 3.536 eV line up at initial-state energy -1.65 eV (marked by the vertical line 2). The increases observed in each of the curves for $\hbar\omega \leq 2.604$ eV (including the field-emission curve) as the initial-state energy decreases below -0.5 eV probably correspond to the high-energy tails of peaks situated in the vicinity of -1.65 eV. Since the structures marked by the vertical line 2 do not line up with comparable structures at the same final-state energy in the curve for any other photon energy (as indicated in Fig. 6 by the vertical arrows labeled 2), they presumably reflect a feature of the surface density of states at the initial energy of the transition, i.e., 1.65 eV below E_F . Unfortunately, it is not possible to further verify this by extending the data for $\hbar\omega \leq 2.604$ eV to lower energy because, as $\hbar\omega$ decreases, the signal falls off more rapidly with decreasing energy

and any such structure would be swamped by noise due to electron-electron and electron-wall scattering within the lens-analyzer system.

The remaining structures in the photofield-emission enhancement factors of Fig. 5 (marked by the vertical arrows labeled 3) do not line up with comparable structures at the same initial-state energies in any other enhancement factor. However, Fig. 6 shows that they line up at the same final-state energy of 2.46 eV relative to E_F (marked by the vertical line 3). This indicates that they reflect a feature of the surface density of states at the final energy of the transition, 2.46 eV above E_F .

B. Enhancement factors for copper overlayers on the W(111) surface

Figure 7 shows how the field-emission enhancement factor for the (111) facet changes as a function of the coverage θ of copper adsorbed at 300 K. Figures 8 and 9 show the corresponding changes in the photofield-emission enhancement factors for photon energies of 2.604 and 3.049 eV, respectively. Data are given only for values of θ up to approximately two monolayers because at higher coverage the copper atoms aggregate to form islands. A peak in the clean-surface ($\theta=0$) curves is observed at approximately the same initial-state energy (-0.69 eV) as in previous studies of field emission,²⁸ surface photofield emission,² and ARUPS (Ref. 29) from the W(111) surface. Structure observed in field-emission data from tungsten in this energy range has previously been attributed to emission from high surface density of states regions associated with the bottom of bulk energy bands at the Γ_7^+ point at the Brillouin-zone center.³⁰ However,

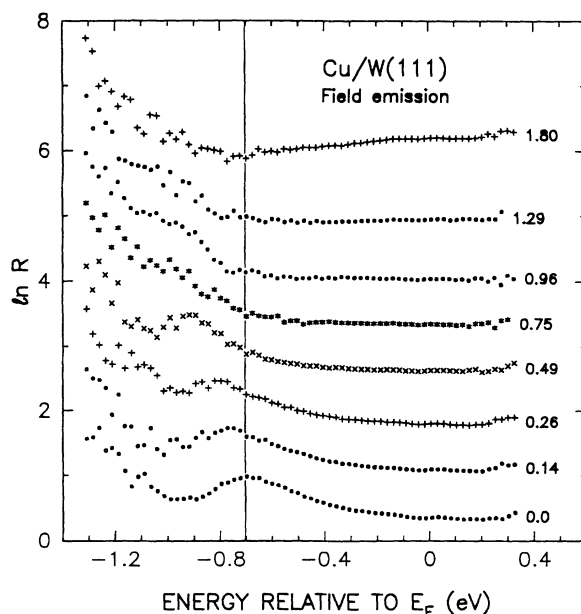


FIG. 7. Field-emission enhancement factor as a function of copper coverage θ on the W(111) facet at 300 K. The plotting conventions are defined in the caption to Fig. 1. The vertical line marks the energy of the peak (-0.69 eV) for the clean surface.

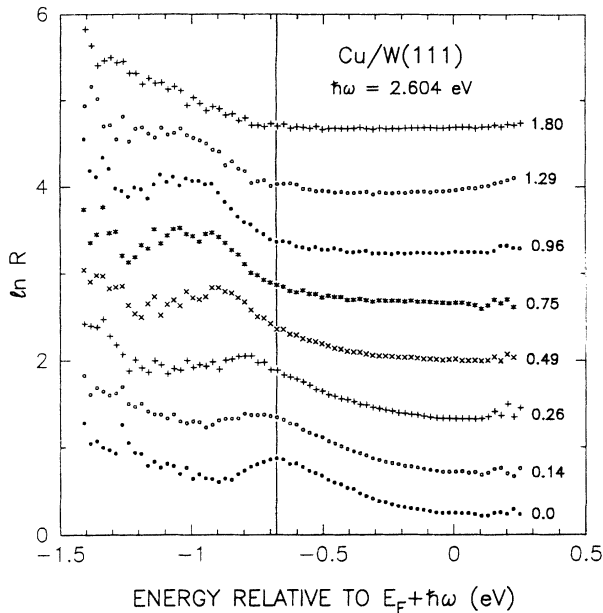


FIG. 8. Enhancement factor in photofield emission in p polarization for $\hbar\omega = 2.604 \text{ eV}$ as a function of copper coverage θ on the W(111) facet at 300 K. The plotting conventions are defined in the caption to Fig. 1. The vertical line marks the energy (-0.69 eV) of the peak for the clean surface.

more recent photoemission measurements have interpreted this structure as arising from a surface state.³¹ Adsorbed copper produces qualitatively similar changes in the field-emission and in the photofield-emission enhancement factors. However, in contrast to copper adsorption on the (100) facet, no additional structure appears at high

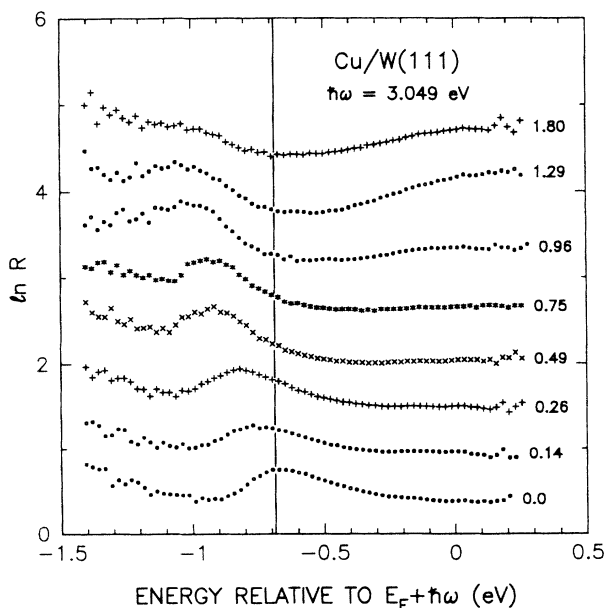


FIG. 9. Enhancement factor in photofield emission p polarization for $\hbar\omega = 3.049 \text{ eV}$ as a function of copper coverage θ on the W(111) facet at 300 K. The plotting conventions are defined in the caption to Fig. 1. The vertical line marks the energy (-0.69 eV) of the peak for the clean surface.

coverage.

As the coverage θ increases, the peak 0.69 eV below $E_F + \hbar\omega$ shifts to lower energy, with no significant reduction in amplitude until θ reaches approximately one monolayer. Beyond one monolayer the peak does not shift further in energy, but its amplitude decreases with increasing θ . The peak remains visible up to the highest θ investigated (1.80 monolayers), being most prominent in the data for $\hbar\omega = 3.049 \text{ eV}$. The peak is superimposed on a background that is generally constant for energies above the peak, but that increases with decreasing energy below the peak. Near one monolayer coverage, the enhancement factors are all essentially constant over the energy range between -0.8 and 0.3 eV , indicating that the calculated free-electron TED satisfactorily represents the energy dependence of the experimental TED over quite a wide range of initial-state energies. Some of the enhancement factors at the higher coverages have an overall positive slope, which might indicate a failure of the classical image potential to describe the form of the surface barrier under those conditions.

Figure 10 compares enhancement factors measured in field emission and in photofield emission using photon energies of 2.604 and 3.049 eV for 0.96 monolayers of copper on the (111) facet. The peaks in the different curves line up at an initial-state energy 0.96 eV below E_F , marked by the vertical line. This is approximately 0.27 eV lower than the energy of the corresponding feature on the clean W(111) surface.

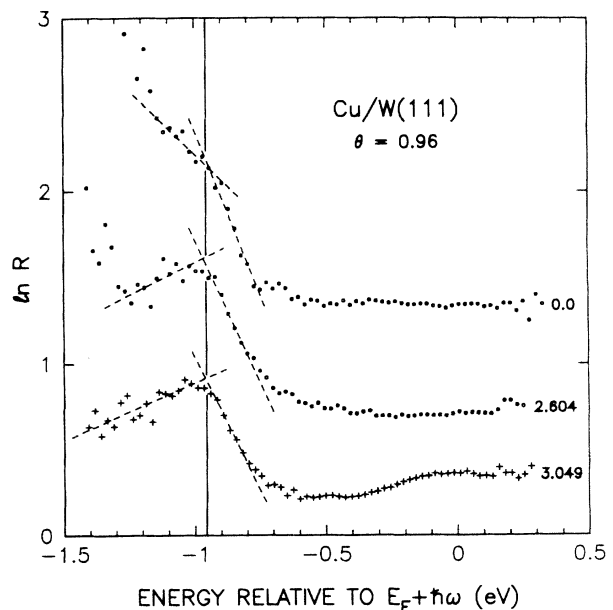


FIG. 10. Enhancement factors in field emission and in photofield emission in p polarization for 0.96 monolayers of copper chemisorbed on the W(111) facet at 300 K. The plotting conventions are defined in the caption to Fig. 5. The vertical line marks the mean energy (-0.96 eV) of qualitatively similar structures.

IV. DISCUSSION

A. Effect of copper overlayers on the surface states of W(100)

The TED's measured on the (100) facet of a tungsten field emitter in field emission and in photofield emission demonstrate that copper adsorption at 300 K reduces the amplitude of the prominent peak (situated at an initial-state energy 0.35 eV below E_F) associated with emission from the higher-energy band of W(100) surface states. The peak gradually weakens as the coverage θ increases in the first monolayer, and is so weak at the highest value of θ investigated (0.96 monolayers) that it can be resolved only in photofield emission at the highest available photon energy (3.536 eV). Studies of copper adsorption on W(100) surfaces of macroscopic size show that, in the present experimental conditions, copper atoms bond to the W(100) surface at the centers of four adjacent tungsten atoms, thereby forming a (1×1) overlayer at one-monolayer coverage.^{26,27} Assuming that the Cu-W bonds formed are sufficiently strong to locally destroy the surface band, a complete overlayer would be expected to obliterate the band everywhere on the surface. This is consistent with the present observation that a nearly complete monolayer of copper effectively quenches all emission from the surface band.

The view that chemisorbed copper effectively destroys the higher-energy band of surface states on the W(100) surface is consistent with the ARUPS data obtained by Attard and King¹⁰ at normal electron emission on macroscopic W(100) surfaces, both for copper adsorption at 300 K and for adsorption at 300 K followed by annealing at 800 K. Their spectra for adsorption without annealing indicate that emission from the surface band progressively decreases as θ increases in the first monolayer, and that it is completely quenched when θ reaches almost one monolayer. For annealed deposits they find that the emission decreases more rapidly with increasing θ and that quenching occurs at a lower value of θ near 0.5 monolayers. There is no evidence in either case for reemergence of emission from the surface band as θ increases after quenching.

The differences between the ARUPS data for nonannealed and annealed deposits are attributed to the different structures of the adsorbate.¹⁰ On macroscopic W(100) surfaces, copper adsorption at 300 K without annealing yields the conventional (1×1) overlayer structure that covers the surface at $\theta = 1$ monolayer,^{26,27} whereas annealing at an elevated temperature induces a two-dimensional surface alloy in which copper atoms partially replace tungsten atoms in the surface layer in a $c(2 \times 2)$ structure that covers the surface by $\theta = 0.5$ monolayers.²⁷ Thus emission from the surface band is quenched when the copper atoms completely cover the W(100) surface in the appropriate configuration, i.e., at $\theta = 1$ and 0.5 monolayers for nonannealed and annealed deposits, respectively.

The effect of adsorbed copper on the higher-energy surface band on the W(100) surface has also been investigated previously using field emission. Richter and Go-

mer⁷ report that the emission from this band is completely quenched at all θ above 0.5 monolayers, both for adsorption at 20 K and for adsorption at 20 K followed by annealing at 300 K. Jones and Roberts,⁸ examining adsorption at 78 K, also find the emission from the higher-energy surface band to be quenched when θ reaches approximately 0.5 monolayers. While these studies suggest that chemisorbed copper destroys the surface band, in agreement with the present findings, they also indicate that the quenching is complete before a monolayer is formed.

The more rapid quenching observed by Richter and Gomer⁷ and by Jones and Roberts⁸ can be reconciled with the present observations if the previous experimental conditions resulted in the clean areas of the W(100) surface being effectively eliminated at lower θ . The low temperatures used in the previous studies^{7,8} tend to inhibit diffusion of the adsorbate, favoring the formation of random (disordered) distributions, whereas the higher temperature used in the present experiments may lead to distributions having more short-range order, i.e., to (1×1) islands. At a given submonolayer coverage θ , a random distribution of copper atoms might be expected to interact with a greater number of tungsten (substrate) atoms, and thus affect the surface band over a larger area of the surface. The results obtained by Richter and Gomer⁷ for annealed submonolayer deposits are more difficult to explain, since the effect of heating to 300 K on the initially random distribution of chemisorbed copper atoms is not known.

The field-emission results of Billington and Rhodin⁹ for adsorption at 78 K exhibit larger discrepancies. They find that very small deposits of copper ($\theta < 0.25$ monolayers) are sufficient to completely quench all emission from the higher-energy surface band, and that emission from this band reemerges, though with considerably reduced intensity, at one-monolayer coverage. The emission disappears on further increasing θ , but reemerges once again at two-monolayers coverage.

It is difficult to account for the discrepancies between the findings of Billington and Rhodin⁹ and those of the other investigations (including the present one). A known difference is the use by these authors of a field-evaporated tungsten tip, which results in a W(100) surface that is more perfectly formed and free of defects than those found on a thermally annealed tip or a macroscopic specimen. Interestingly, field-emission results obtained by Billington¹² for copper adsorption on the W(111) surface under conditions similar to those used in the Billington-Rhodin experiments⁹ agree reasonably well, as will be discussed below, with the (111) data reported here both in field emission and in photofield emission. It might be expected that the loosely packed structure of the W(111) surface is less sensitive to the differences between field-evaporated and thermally annealed tips.

Billington and Rhodin⁹ interpreted their results for copper adsorption, and similar findings for gold, in terms of the relationship between the structures of the overlayer and the substrate. Calculations by Kar and Soven³² had previously demonstrated that a $c(2 \times 2)$ overlayer of

krypton on the W(100) surface quenches the surface-state peak, whereas a (1×1) overlayer of gold, in spite of its stronger electron-scattering properties, does not. Drawing on these results, Billington and Rhodin suggested that so long as the adsorbed atoms present the field-emitted electrons with a potential not very different from that of the tungsten (substrate) atoms, and so long as the transverse symmetry of the substrate is preserved, i.e., a (1×1) overlayer is formed, field emission from a given surface state might not be quenched. Thus they accounted for the observed pattern of quenching and reemergence of the W(100) surface-state peak in their field-emission data during both copper and gold adsorption by arguing that their experiments produced disordered overlayers at fractional coverage, and ordered (1×1) overlayers at $\theta=1$ and 2 monolayers.

At the time when Kar and Soven³² performed their calculations, the W(100) surface-state peak was believed to originate from what is now understood to be the lower-energy band of surface states on the W(100) surface.⁵ Their results do not, therefore, describe the effect of adsorption on the surface-state peak, since it originates from the higher-energy surface band, but instead describe the effect on the weak structure in the field-emission TED situated approximately 0.75 eV below E_F . Since the lower-energy band exists only for nonzero transverse wave vectors, whereas the higher-energy band exists even at zero transverse wave vector, the calculations of Kar and Soven may not correctly give even the qualitative effect of adsorption on the surface-state peak. Moreover, contrary to the prediction of Kar and Soven's calculations, the present field-emission data yield no conclusive evidence for emission from the lower-energy surface band for nearly one monolayer of copper on the W(100) surface. Following the argument of Billington and Rhodin,⁹ this suggests that the potential in the copper overlayer differs sufficiently from that in the tungsten surface layer to destroy the surface band.

B. Effect of copper overlayers on the surface states of W(111)

The TED's measured on the (111) facet both in field emission and in photofield emission demonstrate that adsorbing up to one monolayer of copper does not significantly attenuate the surface-state peak that is situated 0.69 eV below E_F on the clean W(111) surface. However, increasing the coverage θ in this range causes a continuous shift of the peak to lower energy, with a maximum shift of 0.27 eV near one monolayer. As θ increases in the second monolayer, the peak gradually weakens without any further shift in energy, but even at the highest coverage investigated (1.80 monolayers) it can still be resolved in photofield emission at the highest photon energy (3.049 eV). Under the present experimental conditions, copper atoms adsorbed at the W(111) surface presumably occupy the hollows formed by three adjacent tungsten atoms of the surface layer and one tungsten atom of the subsurface layer, thereby forming a (1×1) overlayer at monolayer coverage. If the Cu-W bonds shift the energies of the states responsible for the peak without destroying them, a complete overlayer would be

expected to shift these states everywhere on the surface. This is consistent with the present finding that the energy of the peak decreases up to a coverage of one monolayer, and that no shift occurs for a further increase in θ .

Field-emission data on the electronic properties of copper adsorbed at 78 and 430 K on the W(111) surface have been reported by Billington.¹² The low-temperature data agree quite well with the present findings in that they also show a peak situated 0.69 eV below E_F on the clean surface, which shifts to lower energy without significant attenuation as θ increases in the first monolayer. The shift reaches 0.2 eV at θ near one monolayer, consistent with the shift of 0.27 eV at $\theta=0.96$ monolayers found in the present work. As θ increases above one monolayer, Billington observed extra weight on the low-energy side of the peak, while the peak decreased in amplitude without shifting appreciably in energy. Apart from the appearance of extra weight, this is consistent with the behavior observed in present study. By contrast, the high-temperature results obtained by Billington are very different from the present findings in that the peak vanishes at θ less than 0.25 monolayers and that an additional structure emerges near 0.8 eV below E_F during the formation of the second overlayer. While the authors know of no other data on the electronic structure of copper chemisorbed on the W(111) surface, similar shifts in energy have been observed for surface states of the substrate in other adsorption systems.³³

C. Surface electronic structure of copper overlayers on W(100)

The data for the (100) facet indicate that the first monolayer of chemisorbed copper introduces additional features in the surface density of states. As the coverage θ increases in the first monolayer, adsorbate-induced features 1.65 eV below E_F and 2.46 eV above E_F grow progressively in strength, becoming most prominent in the data for $\theta=0.96$ monolayers (Figs. 5 and 6). Previous results in field emission⁷⁻⁹ and in ARUPS (Ref. 10) do not, however, indicate the presence of these peaks. Moreover, these previous investigations found additional surface densities-of-states features for submonolayer coverages of copper on the W(100) surface that are not observed in the present work.

The peak 2.46 eV above E_F could not have been detected in the earlier field-emission studies because it lies far above the range of energies accessible in such measurements. The other discrepancies are more difficult to explain, but they might originate from known differences in the preparation of the copper overlayer mentioned above in connection with the quenching of the W(100) surface states. These differences could lead to different distributions of copper atoms over the array of possible adsorption sites, which might collectively possess different electronic properties. In any event, Jones and Roberts⁸ could not have detected the peak 1.65 eV below E_F because they measured the field-emission TED using a retarding potential energy analyzer. Typically, the large shot noise associated with this type of analyzer limits the range of energies accessible below the Fermi level to well within 1 eV of E_F , thereby making detection of even the high-

energy side of the peak extremely difficult.

While the structure 2.46 eV above E_F also lies outside the range of energies accessible in ARUPS measurements, the peak 1.65 eV below E_F should be manifest in ARUPS data for copper on W(100). Attard and King¹⁰ observed a peak approximately 1.5 eV below E_F in spectra obtained at normal electron emission for adsorption at 300 K. However, their peak, which exists even for the clean (100) surface and is not appreciably affected by up to 2.5 monolayers of chemisorbed copper, was attributed to emission from the tungsten $5d$ band. Their data also demonstrate clearly that emission from the $3d$ band of the copper overlayer lies well below the energy range investigated in the present study. Emission from the tungsten $5d$ band is suppressed in the present experiments because the relevant wave functions are sufficiently localized that their overlap with the tails of vacuum wave functions in the surface barrier region is negligible.³⁴

Interestingly, when adsorbing either silver or gold on W(100) at 300 K, Attard and King¹⁰ observed, in addition to the overlayer d band, an extra peak situated 2–3 eV below E_F that is prominent only at coverages near one monolayer. This peak, which lies between the substrate and the overlayer d bands, was attributed to emission from interface states. They found no such peak for copper adsorption at 300 K, perhaps because the corresponding interface state for the copper overlayer lies sufficiently close in energy to the tungsten $5d$ bands that emission from it cannot be distinguished from d -band emission. The peak observed 1.65 eV below E_F in the present field-emission and photofield-emission data for approximately one monolayer of copper on the W(100) surface may originate from an interface state similar to those seen at slightly lower energies by Attard and King¹⁰ for silver and gold overlayers. The fact that the coverage dependence of the peak observed 2.46 eV above E_F is similar to that of the lower-energy peak suggests that it too might originate from an interface state.

Further progress in understanding the origin of the copper-induced peaks must await accurate calculations of the surface electronic structure for one monolayer of copper adsorbed on the W(100) surface. Self-consistent calculations of this type have been carried out recently for complete (1×1) copper monolayers on W(110) (Ref. 13) and on Ru(0001),³⁵ and for a (1×1) Ni monolayer on Ru(0001).³⁶ In each case, the adsorption system is modeled as a five-layer substrate slab with (1×1) adlayers on the two exposed surfaces, and the surface electronic structure is calculated semirelativistically using the linearized augmented plane wave (LAPW) method. The effects of exchange and correlation are represented by a local-density-functional exchange-correlation potential. For each system, the calculations indicate bands of states below the Fermi level that are either localized on the adlayer (surface states) or shared between the adlayer and the first substrate layer (interface states). The dispersion behavior for these bands corresponds well to that of bands detected in ARUPS measurements along selected symmetry lines in the substrate surface Brillouin zone.^{13,35,36} Furthermore, the calculated surface or interface character of the states is consistent with that in-

ferred from ARUPS data as a function of the adsorbate coverage.

For a monolayer of copper adsorbed on the W(110) surface, discrepancies of a few tenths of an electron volt exist between the experimental and the calculated binding-energy values for some of the surface and/or interface states. These discrepancies have been attributed to the neglect of spin-orbit coupling in the LAPW calculations,¹³ which can be important in tungsten. Nevertheless, the overall agreement for the dispersion behavior and for the surface or interface character of the states is satisfactory. The above considerations suggest that analogous calculations of the surface electronic structure for a (1×1) copper monolayer on the W(100) surface might go a long way towards identifying the origin of the copper-induced surface densities-of-states features in the present (100) data near monolayer coverage. Self-consistent slab calculations have already been carried out both for the clean W(100) surface⁶ and for a $c(2 \times 2)$ cesium overlayer.³³ In addition to any information on copper-induced states, such calculations might also help explain the quenching of emission from the W(100) surface states by a copper overlayer.

Studies of surface photofield emission from clean tungsten have yielded no evidence for structure due to the surface density of states at the final energy of the transition.² The emission current has been attributed entirely to photoexcitations from occupied electronic states whose wave functions have appreciable amplitude just outside the metal to a continuum of free-electron-like tunneling states of the vacuum.^{2,37} Photofield-emission data for approximately one monolayer of copper chemisorbed on the W(100) facet show clear evidence of structure 2.46 eV above E_F at the final energy of the transition (Fig. 6). Final-state structure has also been observed in surface photofield emission from the center of an aggregate of copper atoms chemisorbed on the W(110) surface.¹⁷ These observations show that surface and interface states of the adsorbed overlayer can act as final states for surface photoexcitation. The present results demonstrate that this technique can provide useful information on the surface density of states of adsorbed overlayers in the energy range between the Fermi level and the vacuum level.

V. CONCLUSIONS

Field-emission and surface photofield-emission measurements have shown that spatially homogeneous overlayers of copper chemisorbed on the (100) and (111) facets of a thermally annealed tungsten field emitter substantially modify the surface electronic structure of the substrate. On the (100) facet, a submonolayer coverage of copper suppresses the higher-energy band of W(100) surface states with no appreciable shift in energy, quenching it completely when the coverage reaches one monolayer. By contrast, adsorbing copper on the (111) facet shifts the W(111) surface state to lower energy with no appreciable attenuation. Above one monolayer, the surface state decreases in intensity with no further shift in energy. These findings offer insight into the conflicting results of previous work.

On the (100) facet, submonolayer coverages of copper introduce additional features in the surface density of electronic states, which become most prominent near one monolayer. On the (111) facet, by contrast, no additional features are detected for up to two monolayers of adsorbed copper. On the (100) facet, a copper-induced feature is detected at the final-state energy in surface photofield emission, demonstrating that this technique can provide useful information on the surface density of states of an adsorbed overlayer in the energy range between the Fermi level and the vacuum level. It is hoped that the present results will serve as a guide for future

theoretical descriptions of the surface density of states at copper-tungsten interfaces.

ACKNOWLEDGMENTS

The authors wish to acknowledge the technical assistance of K. Weisser of the Scarborough College Academic Workshops. This work was supported in part by operating and equipment grants from the Natural Sciences and Engineering Research Council (NSERC) of Canada.

-
- ¹L. W. Swanson and L. C. Crouser, *Phys. Rev. Lett.* **16**, 389 (1966).
²D. Venus and M. J. G. Lee, *Surf. Sci.* **172**, 477 (1986).
³Y. Gao and R. Reifenberger, *Phys. Rev. B* **32**, 1380 (1985).
⁴B. J. Waclawski and E. W. Plummer, *Phys. Rev. Lett.* **29**, 783 (1972).
⁵S.-L. Weng, E. W. Plummer, and T. Gustafsson, *Phys. Rev. B* **18**, 1718 (1978); M. J. Holmes and T. Gustafsson, *Phys. Rev. Lett.* **47**, 443 (1981).
⁶M. Posternak, H. Krakauer, A. J. Freeman, and D. D. Koelling, *Phys. Rev. B* **21**, 5601 (1980); L. F. Mattheiss and D. R. Hamann, *ibid.* **29**, 5372 (1984).
⁷L. Richter and R. Gomer, *Surf. Sci.* **83**, 93 (1979).
⁸J. P. Jones and E. W. Roberts, *Surf. Sci.* **64**, 355 (1977).
⁹R. L. Billington and T. N. Rhodin, *Phys. Rev. Lett.* **41**, 1602 (1978).
¹⁰G. A. Attard and D. A. King, *Surf. Sci.* **222**, 351 (1989).
¹¹P. L. Young and R. Gomer, *Surf. Sci.* **44**, 268 (1974); L. Richter and R. Gomer, *ibid.* **59**, 575 (1976); G. Lilienkamp, C. Koziot, and E. Bauer, *ibid.* **226**, 358 (1990).
¹²R. L. Billington, Ph.D. thesis, Cornell University, Ithaca, NY, 1981.
¹³J. E. Houston, P. J. Feibelman, D. G. O'Neill, and D. R. Hamann, *Phys. Rev. B* **45**, 1811 (1992).
¹⁴D. R. Penn and E. W. Plummer, *Phys. Rev. B* **9**, 1216 (1974).
¹⁵G. A. Gaudin and M. J. G. Lee, *Surf. Sci.* **280**, 91 (1993).
¹⁶G. A. Gaudin, Ph. D. thesis, University of Toronto, Toronto, 1993.
¹⁷G. A. Gaudin and M. J. G. Lee, *Surf. Sci.* (to be published).
¹⁸D. Venus and M. J. G. Lee, *Rev. Sci. Instrum.* **56**, 1206 (1985).
¹⁹P. J. Donders, K. W. Hadley, and M. J. G. Lee, *Rev. Sci. Instrum.* **56**, 2074 (1985).
²⁰D. Venus and M. J. G. Lee, *Surf. Sci.* **125**, 452 (1983).
²¹R. D. Young, *Phys. Rev.* **113**, 110 (1959).
²²C. Schwartz and M. W. Cole, *Surf. Sci.* **115**, 290 (1982).
²³H. Q. Nguyen, P. H. Cutler, T. E. Feuchtwang, N. Miskovsky, and A. A. Lucas, *Surf. Sci.* **160**, 331 (1985).
²⁴J. W. Gadzuk and E. W. Plummer, *Rev. Mod. Phys.* **45**, 487 (1973); R. W. Strayer, W. Mackie, and L. W. Swanson, *Surf. Sci.* **34**, 225 (1973).
²⁵G. A. Gaudin and M. J. G. Lee, *Surf. Sci.* **185**, 283 (1987).
²⁶E. Bauer, H. Poppa, G. Todd, and F. Bonczek, *J. Appl. Phys.* **45**, 5164 (1974).
²⁷G. A. Attard and D. A. King, *Surf. Sci.* **188**, 589 (1987).
²⁸J. W. Gadzuk and E. W. Plummer, *Phys. Rev. Lett.* **25**, 1439 (1970); E. W. Plummer and A. E. Bell, *J. Vac. Sci. Technol.* **9**, 583 (1972).
²⁹B. Feuerbacher and N. E. Christensen, *Phys. Rev. B* **10**, 2373 (1974).
³⁰E. W. Plummer, in *Interactions on Metal Surfaces*, edited by R. Gomer (Springer, New York, 1975).
³¹F. Cerrina, J. R. Anderson, G. J. Lapeyre, O. Bisi, and C. Calandra, *Phys. Rev. B* **25**, 4949 (1982).
³²N. Kar and P. Soven, *Solid State Commun.* **20**, 977 (1976); N. Kar, *Surf. Sci.* **70**, 101 (1978).
³³P. Soukiassian, R. Riwan, J. Lecante, E. Wimmer, S. R. Chubb, and A. J. Freeman, *Phys. Rev. B* **31**, 4911 (1985).
³⁴J. W. Gadzuk, *Phys. Rev.* **182**, 416 (1969).
³⁵J. E. Houston, C. H. F. Peden, P. J. Feibelman, and D. R. Hamann, *Phys. Rev. Lett.* **56**, 375 (1986); *Surf. Sci.* **192**, 457 (1987).
³⁶J. E. Houston, J. M. White, P. J. Feibelman, and D. R. Hamann, *Phys. Rev. B* **38**, 12164 (1988).
³⁷G. P. Lopinski, P. J. Donders, and M. J. G. Lee, *Surf. Sci.* **201**, 294 (1988).